Project 2
A new Class of Solar Cells
Studying α-$CsPbI_3$ using DFT

Ritesh Balayan

Abstract

Density functional theory (DFT) is a widely used method for calculating electronic properties of materials. In this study, we employed the quantum espresso software package to investigate the band gap of alpha CsPbI3, a promising material for solar cell applications. Due to the inherent difficulty in accurately determining band gaps in DFT, we tested four different exchange-correlation functionals: GGA, PBE, PBEsoc, and vdw-DF2. Our results show that vdw-DF2 provides the best agreement with experimental data and is therefore the most suitable functional for exploring the solar properties of CsPbI3. This study highlights the importance of selecting appropriate exchange-correlation functionals in DFT calculations and provides insights into the electronic properties of CsPbI3 that can aid in the development of efficient solar cells.

Keywords: Density Functional Theory, Solar Cell, Persikovites, Band gap Calculation.

1. Theory

1.1. Density Functional Theory

DFT is a theoretical framework for describing the electronic structure of materials. In this approach, the system's total energy is expressed as a functional of the electron density. This functional is minimized to obtain the ground state energy and electron density. DFT is based on assumption that all the physical and chemical properties can be determined from this ground state Density. The exchange-correlation (XC) functional is a fundamental component of DFT and describes the interactions between electrons in a material.

The exchange term arises from the fact that electrons are identical particles and must obey the Pauli exclusion principle, which states that no two electrons can occupy the same quantum state simultaneously. The exchange energy is the energy associated with the exchange of two electrons in a system. The exact form of the XC functional is unknown and must be approximated in practice.

1.2. Perovskites

Perovskites are a class of materials that have a crystal structure similar to that of calcium titanium oxide mineral perovskite, with the general chemical formula ABX3. The unique properties of perovskites, such as their high tunability, flexibility, and ease of processing, make them highly attractive for a range of applications, including solar cells, light-emitting diodes (LEDs), photodetectors, and lasers.

Additionally, perovskites are highly flexible in terms of their composition, with various combinations of A, B, and X elements possible. This means that perovskites can be tailored for specific applications by tweaking the chemical composition of the material, giving rise to a vast array of potential uses.

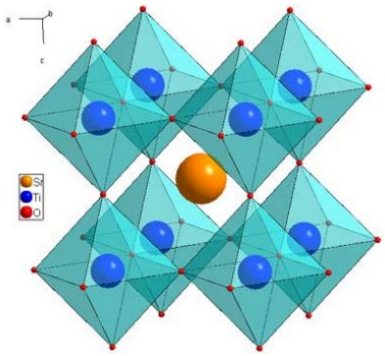

Figura 1: Cubic crystal structure of perovskite SrTiO3. Taken from https: //www.princeton.edu/ cavalab/tutorials/public/structures/ perovskites.html.

Now, alpha-CsPbI3 is an important perovskite to study because it has shown promising potential for use in highly efficient solar cells. Alpha-CsPbI3 is a specific form of the CsPbI3 perovskite that has a unique crystal structure, which is highly desirable for solar cell applications due to its excellent optoelectronic properties.

2. Aim

The aim of this project is to determine the appropriate cutoff energy and Kpoint Grid to achieve convergence and find appropirate ground state electron density, followed by a comparison of the Density of States (DOS) and band structure of different

correlation functionals to experimental data. The ultimate goal is to identify the parameters that best match the experimental results. The experimental data will be referenced to the paper[3], while the optimized geometry will be referenced to the paper [3]. Experimental Bandgap of 1.68 eV will be refered as experimental value in this report. And optimised geometry is simple cubic lattice with cube dimention 12.0675 au. with the cell diagram depicted in Figure 2. The input for Quantum Espresso is provided in Figure 3.

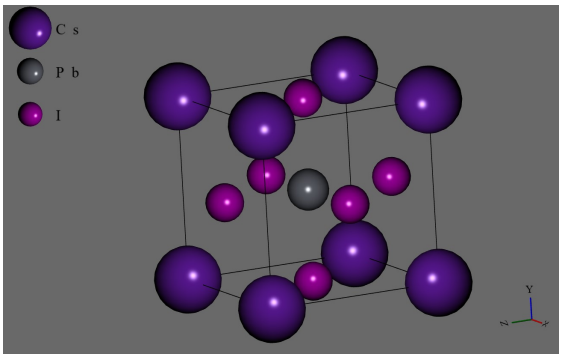

Figura 2: Visualisation Of Unit Cell Used for Calculation

```
 &control
    calculation='scf'
    restart_mode='from_scratch',
    prefix='cspbi3',
    pseudo_dir = './',
    outdir='cspbi3-a/'
 /
 &system
! Enter crystal structure information below
    ibrav= 1
    celldm(1) = 12.067675236
    ntyp= 3
    nat= 5
! Edit plane wave cutoff below if necessary
    ecutwfc = 60.0,
    occupations='tetrahedra',
 /
 &electrons
    conv_thr =  1.0d-7
    mixing_beta = 0.7
 /
ATOMIC_SPECIES
Cs  132.9 Cs.pz-hgh.UPF
Pb  207.2 Pb.pz-hgh.UPF
I   126.9  I.pz-hgh.UPF

ATOMIC_POSITIONS
 Cs 0.00 0.00 0.00
 Pb 0.50 0.50 0.50
 I  0.50 0.50 0.00
 I  0.50 0.00 0.50
 I  0.00 0.50 0.50


K_POINTS {automatic} ! Edit k-point grid size below
 8 8 8    0 0 0
```

Figura 3: Input file for SCF calculation used in quantum espresso

3. Convergence

The project's primary objective is to achieve convergence in the self-consistent field (SCF) calculation by varying K points and cutoff energy. As shown in Figure 4, we studied convergence by adjusting the K point grid and cutoff energy. Our findings indicate that with the chosen resolution, the cutoff energy is a more crucial parameter in achieving convergence. The curves in Figure 5d are significantly more divergent than those in Figure 5c, illustrating this point. The total energy is measured in Ry/Cell. Our goal is to achieve convergence at 5 meV/Atom.

After analyzing the data, we determined that the cell with an 8x8x8 Kpoint and a cutoff energy of 60 Ry was the first cell to converge with respect to both parameters within the desired accuracy. We concluded that 60 Ry cutoff energy and an 8x8x8 Kgrid can be used for further calculations, as convergence has been achieved.

Cut off Energy	Column2	Column3	Column4	Column5	Column6	Column7	Column8	
Kgrid(NxNxN)	4	6	8	10	12	14	16	Total Energy in Ry/Cell
20	-77.20362541	-77.20641887	-77.2067219	-77.20680516	-77.20676605	-77.20678356	-77.20681669	
30	-77.26758345	-77.27022214	-77.27051363	-77.27056491	-77.27056336	-77.27056701	-77.27056604	
40	-77.27641962	-77.27910619	-77.27939201	-77.27943251	-77.27943651	-77.27943836	-77.2794394	
50	-77.27918973	-77.28187385	-77.28216003	-77.2821999	-77.28220611	-77.28220753	-77.28220751	
60	-77.27980661	-77.28249013	-77.28277546	-77.2828152	-77.28282163	-77.28282283	-77.28282308	
70	-77.2799102							
80	-77.27992644							
90	-77.27993006							
100	-77.27993137							

Figura 4: Convergence Results of total energy at different Kpoint and cutoff energy

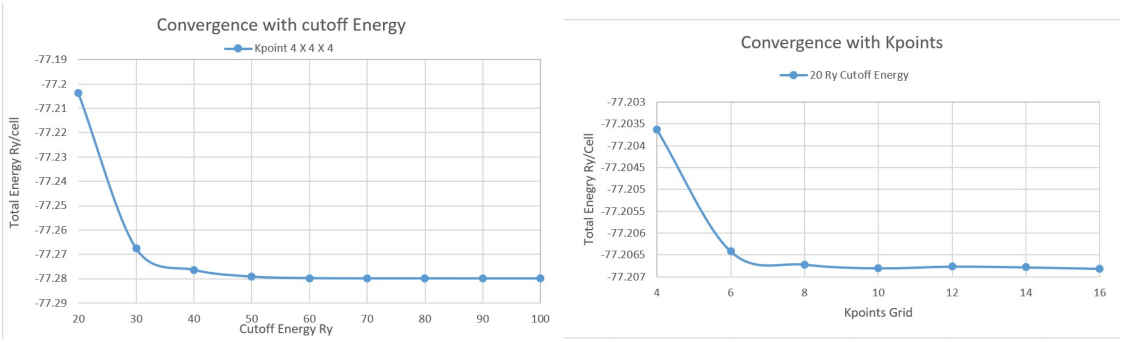

(a) (b)

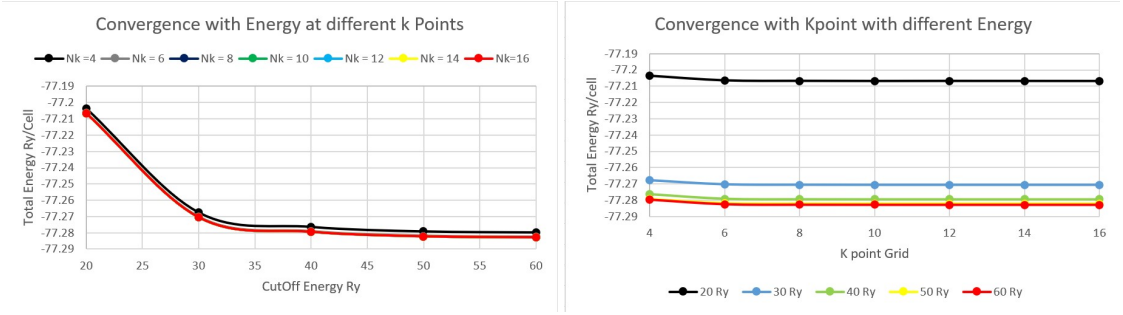

(c) (d)

Figura 5: Plots of total Energy convergence

4. DOS Convergence and Bands

Now that SCF convergence has been achieved, the next step is to perform a non-self-consistent field (NSCF) calculation, followed by Density of State (DOS) plots. We will gradually increase the K points in the NSCF calculation until convergence is achieved in the DOS plots. However, we will not use an excessive amount of computational resources for this step, as our primary goal is to determine the Band gap. Our approach to finding convergence will involve a subjective understanding, where we determine that convergence has been reached when the DOS plots exhibit converged Band Gaps.

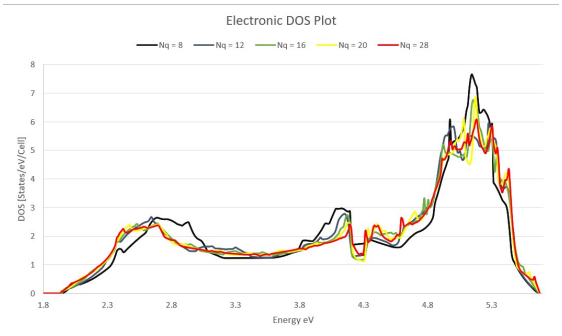

Figura 6: Section of Convergence of DOS with increasing kpoint in non-SCF Calculation see figure 7 for complete DOS with band gap

After both convergence Achieved We plottted the Band Plots along Highly Symmetric Points gamma - R - M. Where we found that bands curves are in aggrement with[1] paper but Band Gaps are off see figure 12.

5. Finding Band Gap Directly From SCF Calculation

Since our primary goal is to determine the Band gap, we do not necessarily need to find the DOS and bands. However, it is still useful to compare our results with the literature. By modifying the script in Quantum Espresso, we were able to determine the Band gap directly from the SCF calculations. We observed that the Band gap calculated in this step was similar to that calculated in the subsequent detailed calculations.

```
 &system
! Enter crystal structure information below
    ibrav= 1,
    celldm(1) = 12.067675236,
    ntyp= 3,
    nat= 5,
    nbnd= 32,
! Edit plane wave cutoff below if necessary
    ecutwfc = 60.0,
    occupations='fixed',
    smearing = "gaussian"
```

```
     highest occupied, lowest unoccupied level (ev):     0.6284    1.9324

!    total energy              =     -77.28282308 Ry
     Harris-Foulkes estimate   =     -77.28282308 Ry
     estimated scf accuracy    <          2.1E-09 Ry

     The total energy is the sum of the following terms:

     one-electron contribution =     -23.10835943 Ry
     hartree contribution      =      18.14896680 Ry
     xc contribution           =     -15.67820897 Ry
     ewald contribution        =     -56.64522148 Ry

     convergence has been achieved in  10 iterations
```

Figura 8: Upper change in input file to extract band gap directly from SCF calculation, occupation is changed to fixed. lower is the band gap information in corrosponding outout file

To determine whether the Band gap was converged, we utili-

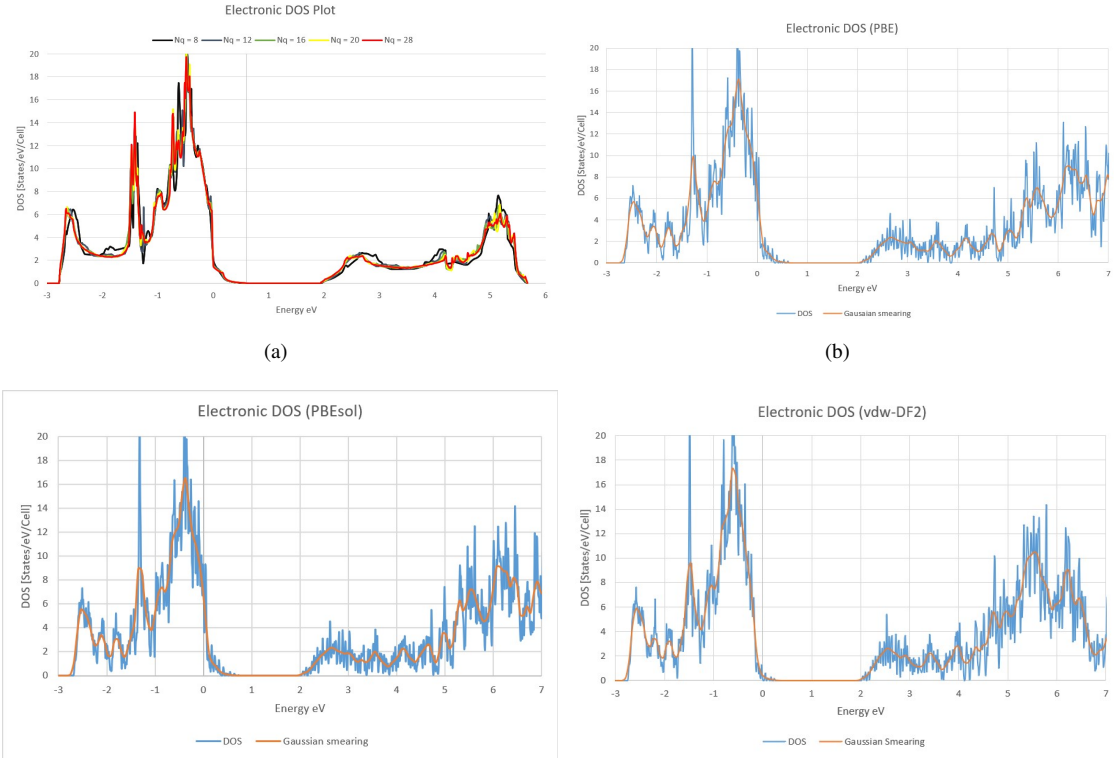

Figura 7: DOS with different exchange correlatinal functional

zed the SCF calculation with the same parameters, K grid of 16 and 20, and cutoff energy of 60 and 70. We found that the Band gap was converged at these K grids and cutoff energies for all four exchange-correlation functionals. Exchange-correlation functional can be changed by input dft parameter in input file. see figure 9 for Detailed converging points.

Bands Gap with Different exchage-correlation Functional							
default xc-functionals				PBE xc-functionals			
bands	32			bands	32		
	cutoff				cutoff		
Kpoint		16	20	Kpoint		16	20
	60	1.304	1.3039		60	1.3956	1.3956
	70	1.304			70	1.3956	
PBEsol xc-functionals				vdw-DF2 xc-functionals			
bands	32			bands	32		
	cutoff				cutoff		
Kpoint		16	20	Kpoint		16	20
	60	1.3123	1.3123		60	1.7157	1.7157
	70	1.3123			70	1.7155	
	Kpoints grid (NxNxN)			Band Gap (eV)		Cutoff energy (Ry)	

Figura 9: Band gap convergence of different xc functional

6. DOS and Bands with Different exchange-corelatinal functional

Next, we obtained the DOS and bands for the three new exchange-correlation functionals, PBE, PBEsol, and vdw-DF2[2]. It is important to note that no NSCF calculations were conducted for these new functionals as SCF calculations were performed on 16 grid points. We plotted all of the DOS and bands together to compare them. While the behavior of all three functionals was similar, their band gap calculations were slightly different. see figure 7 for DOS and figure 12 for Bands.

7. Discussion

Based on our findings, we observed that while all four exchange-correlation functionals converged at the same parameters and had similar DOS and Bands structures, there was a drastic difference in the Band gap values. The default functional (GGA), PBE, and PBEsol functionals produced a Band gap energy of around 1.3 eV, which is off by approximately 30 percent compared to the experimental value of 1.7 eV. However, the vdw-DF2 functional was able to achieve an accuracy of close to 1.5 percent within experimental range. The DOS and Bands plots also helped us to identify where this difference was coming from.

Our results are reliable when it comes to the study of α-$CsPbI_3$ for solar properties and these findings can be utilized when altering the efficiency of this material through impurity or doping. Further research could be conducted to explore the impact of impurities or doping on the band gap and other properties of this material. Overall, our study provides valuable insights into the performance of various exchange-correlation functionals in predicting the Band gap of α-$CsPbI_3$.

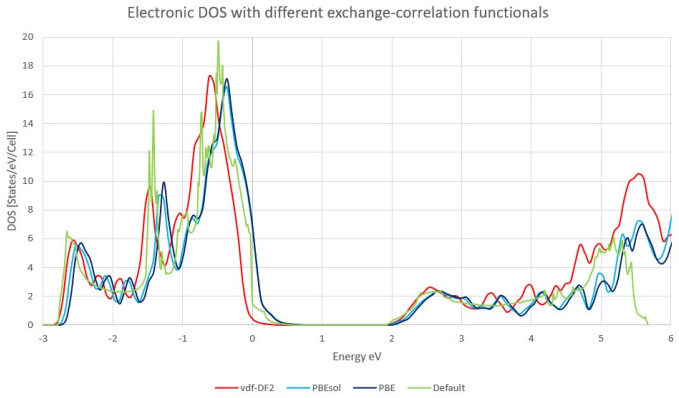

Figura 10: DOS plot all xc functinal overlayed

Figure 12 depicts the density of states (DOS) of all four exchange-correlation (xc) functionals overlaid on each other. It is evident that the peaks of DOS do not align for all functionals. It should be noted that, for the GGA functional, a 28 grid point NSCF calculation was performed, while for PBE, PBEsol, and vdw-DF2, a 16 grid SCF calculation with Gaussian interpolation was used. Figure 7 presents more detailed DOS plots of these functionals.

Figure 11 illustrates a comparison of the band structures of different exchange-correlation functionals. It is observed that the difference in the band gap is amplified at the R point between vdw-DF2 and the GGA functional.

Bands Plots are also found to be similar with bough[1] paper when compared to bands plot of α-$CsPbI_3$.

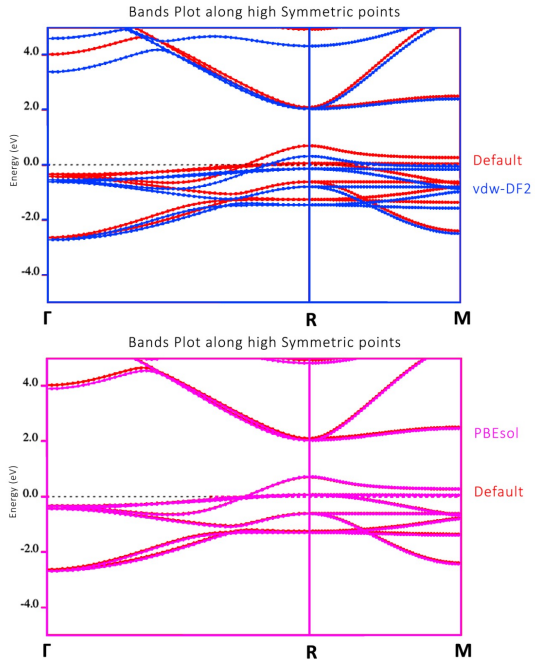

Figura 11: Band plot comparision of default xc functional and vdw-DF2 top and PBEsol with default bottom

8. Conclusion

In conclusion, our study on the structural and electronic properties of α-$CsPbI_3$ has been conducted using Quantum Espresso calculations. We first achieved convergence of the self-consistent field calculation by varying the K-point grid and cutoff energy. We found that a cutoff energy of 60 Ry and an 8x8x8 K-point grid were sufficient for achieving convergence with an accuracy of 5 meV/Atom.

We then proceeded to calculate the density of states and band structures for the α-$CsPbI_3$ using four different exchange-correlation functionals, namely the GGA, PBE, PBEsol, and vdw-DF2. It was observed that all the functionals produced similar structures for the density of states and band structures, but with notable differences in the band gap calculations.

Our results showed that vdw-DF2 exchange-correlation functional was the most accurate in predicting the band gap, with a value of 1.71 eV, which was very close to the experimental value of 1.68 eV. This is in contrast to the other three functionals, which produced band gaps that were off by around 30 percent.

The comparison of the density of states and band structures of the different functionals revealed that the difference in the band gap is amplified at the R point in vdw-DF2 and other functionals bands plot.

Overall, this study has provided valuable insights into the electronic properties of alpha-CsPbI3, and our results are reliable and useful for further study and development of this material for solar properties, especially if efficiency is to be altered by impurity or doping.

Referencias

[1] Jakoah Brgoch, Anna J. Lehner, Michael Chabinyc, and Ram Seshadri. Ab initio calculations of band gaps and absolute band positions of polymorphs of rbpbi3 and cspbi3: Implications for main-group halide perovskite photovoltaics. *The Journal of Physical Chemistry C*, 118(48):27721–27727, 2014.

[2] T. Thonhauser, S. Zuluaga, C. A. Arter, K. Berland, E. Schröder, and P. Hyldgaard. Spin signature of nonlocal correlation binding in metal-organic frameworks. *Phys. Rev. Lett.*, 115:136402, Sep 2015.

[3] Shumao Xu, Alberto Libanori, Gan Luo, and Jun Chen. Engineering bandgap of cspbi3 over 1.7 ev with enhanced stability and transport properties. *iScience*, 24(3):102235, 2021.

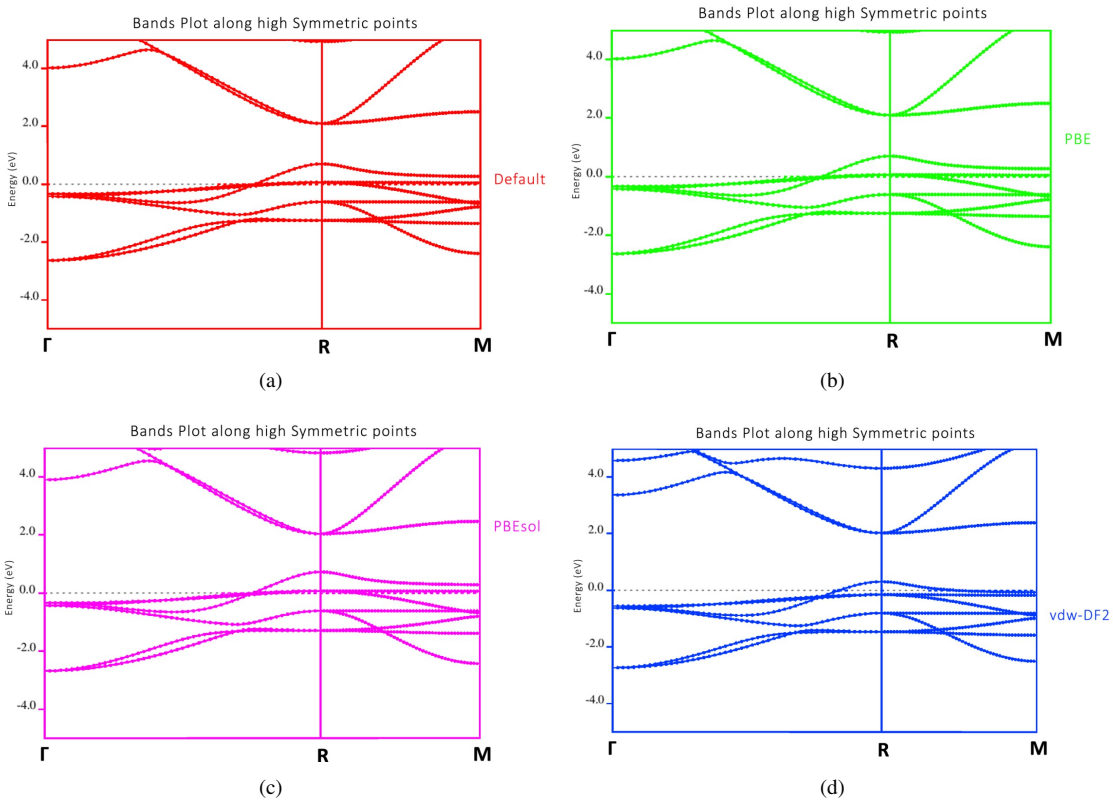

Figura 12: Bands plot of four xc functinal used in project